The scattering of regular surface waves by a fixed, half-immersed, circular cylinder

P. A. MARTIN

Department of Mathematics, University of Manchester, Manchester M13 9PL, UK

A. G. DIXON

Department of Engineering, University of Manchester, Manchester M13 9PL, UK

A train of regular surface waves is incident upon a fixed, half-immersed, circular cylinder; the waves are partially reflected and partially transmitted, and also induce hydrodynamic forces on the cylinder. In order to give a theoretical study of this problem, we make the familiar assumptions of classical hydrodynamics and then solve the linear, two-dimensional, diffraction boundary-value problem, using Ursell's multipole method. Accurate numerical results are presented (in the form of tables) for four important (complex) quantities; these are the reflection and transmission coefficients, and two dimensionless coefficients which describe the horizontal and vertical forces on the cylinder. We have also made an experimental study, in which we measured the forces on the cylinder, and the reflection coefficient. These measurements are compared with the linear theory, and also with other experimental data; discrepancies are noted and an attempt to analyse them is made. We have also measured the mean horizontal forces on the cylinder; these results are compared with the predictions of a simple formula obtained by Longuet-Higgins.

1. INTRODUCTION

Consider a rigid horizontal circular cylinder, of radius a, which is immersed in water. We suppose that the cylinder is fixed, and that a train of regular surface waves is incident upon it. How is such a wave train modified by the cylinder? What are the resulting hydrodynamic forces acting on the cylinder? There is a vast literature which addresses these questions, from both theoretical and experimental viewpoints; for a review, see, e.g. Shaw[1] or Hogben.[2] However, in much of this work, it is assumed that the cylinder is totally submerged; we shall assume that it is only partially immersed. Moreover, we shall only consider the two-dimensional problem, corresponding to beam seas, i.e. waves whose crests are parallel to the axis of the cylinder. Thus, the fluid motion is supposed to be independent of the axial coordinate.

Let d be the vertical distance that the axis of the cylinder is *below* the undisturbed free surface. Thus, when $|d| < a$, the cylinder is only partially immersed. For this configuration, the published experimental data are scarce: Dean and Ursell[3] measured the exciting forces on a half-immersed cylinder ($d = 0$), and also the reflection and transmission coefficients; we shall examine their results in more detail in Section 5. Jeffrey *et al.*[4] have presented many graphs showing the variation of the measured forces (over one cycle) with the frequency and amplitude of the incident wave, and with the depth of immersion ($0.6 \leqslant (d/a) \leqslant 1.6$); they do not consider the case $d = 0$. Dixon *et al.*[5] have measured the vertical force on a cylinder for $0 \leqslant (d/a) \leqslant 1.2$. In order to analyse their data, they developed a modified form of Morison's equation, containing a single 'inertia coefficient' C_M. C_M was determined by fitting their equation to the measured values of the force, over one wave period, and was shown to depend on the frequency and amplitude of the incident wave (and also on d/a). However, it was also shown that a *constant* value of C_M ($C_M = 2.0$) could be used to predict the (vertical) force on the cylinder, with quite good results. For a review of the use of Morison's equation, see, e.g. Hogben *et al.*[6]

In the analysis leading to Morison's equation, it is assumed that the presence of the cylinder does not affect the incident wave, i.e. diffraction effects are ignored. Hogben[2] suggests that Morison's equation is applicable if the diameter of the cylinder ($2a$) is less than $0.2 \times$ wavelength; in our notation (see Section 2), this criterion becomes $Ka < 0.2\pi \simeq 0.6$; at such values of Ka, diffraction effects *are* significant (see Table 1), i.e. a modified criterion is required for horizontal, surface-piercing cylinders.

In this paper, we shall consider only the case of a fixed, half-immersed circular cylinder, in regular waves. In the next section, we idealise the actual physical problem, and formulate the well-known linear boundary-value problems of classical hydrodynamics. For deep water, the scattering problem depends on a single dimensionless parameter, Ka. We have solved this problem, numerically, for $0 < Ka \leqslant 10$, and shall present our results in the form of tables of four important (complex) quantities. These are the reflection coefficient, the transmission coefficient, and two dimensionless coefficients which describe the horizontal and vertical hydrodynamic forces on the cylinder. Although other authors have computed these quantities before, their results (i) are not readily available, (ii) are not all correct, and (iii) are usually presented as graphs – in our opinion, tables are more useful when alternative computer programs (perhaps based on different mathematical methods, or designed to solve more complicated problems) are to be tested and evaluated.

0309-1708/83/010013-11 $2.00

Table 1. Theoretical values for R and T

Ka	$\|R\|$	arg R	$\|T\|$	arg T
0.01	1.965 (−2)	−1.5898	9.998 (−1)	−0.0190
0.02	3.896 (−2)	−1.6073	9.992 (−1)	−0.0365
0.03	5.816 (−2)	−1.6235	9.983 (−1)	−0.0527
0.04	7.734 (−2)	−1.6385	9.970 (−1)	−0.0677
0.05	9.656 (−2)	−1.6524	9.953 (−1)	−0.0816
0.06	1.159 (−1)	−1.6653	9.933 (−1)	−0.0945
0.07	1.353 (−1)	−1.6773	9.908 (−1)	−0.1065
0.08	1.548 (−1)	−1.6884	9.880 (−1)	−0.1176
0.09	1.744 (−1)	−1.6987	9.847 (−1)	−0.1279
0.1	1.942 (−1)	−1.7081	9.810 (−1)	−0.1373
0.2	3.958 (−1)	−1.7678	9.183 (−1)	−0.1970
0.3	5.857 (−1)	−1.7906	8.105 (−1)	−0.2198
0.4	7.369 (−1)	−1.8118	6.760 (−1)	−0.2410
0.5	8.403 (−1)	−1.8550	5.421 (−1)	−0.2842
0.6	9.046 (−1)	−1.9277	4.263 (−1)	−0.3569
0.7	9.427 (−1)	−2.0276	3.337 (−1)	−0.4568
0.8	9.650 (−1)	−2.1495	2.621 (−1)	−0.5787
0.9	9.783 (−1)	−2.2878	2.073 (−1)	−0.7170
1.0	9.862 (−1)	−2.4385	1.655 (−1)	−0.8677
2.0	9.996 (−1)	2.0608	2.663 (−2)	−2.6516
3.0	1.000	0.1315	7.132 (−3)	1.7023
4.0	1.000	−1.8325	2.565 (−3)	−0.2617
5.0	1.000	2.4728	1.117 (−3)	−2.2396
6.0	1.000	0.4877	5.563 (−4)	2.0585
7.0	1.000	−1.5016	3.053 (−4)	0.0693
8.0	1.000	2.7898	1.805 (−4)	−1.9226
9.0	1.000	0.7962	1.131 (−4)	2.3670
10.0	1.000	−1.1986	7.428 (−5)	0.3722

We shall also compare the linear theory with experiment; this is done in Section 5. The details of the experimental techniques and equipment are given in Section 4. We compare the reflection coefficient and the force coefficients, with those predicted by linear theory; various discrepancies are noted, and an attempt is made to analyse them. Finally, we have also measured the mean horizontal forces on the cylinder; we compare these measurements with a simple formula obtained by Longuet-Higgins.[7]

2. MATHEMATICAL FORMULATION

Consider a train of regular surface waves which is incident upon a fixed, half-immersed circular cylinder. We define Cartesian coordinates (x, y) such that the origin is at the centre of the circle, the x-axis is horizontal and points towards the incident wave, and the y-axis is vertical and increases with depth. We suppose that the water is inviscid and incompressible, and neglect the effects of surface tension. For simplicity, we also suppose that the water is of infinite depth. We assume that the motion of the water is irrotational, whence a velocity potential exists. If we further assume that the motion has a harmonic time-dependence (with circular frequency ω), then we may write the velocity potential as the real part of $\phi(x,y)\exp(-i\omega t)$; henceforth, we shall suppress the factor $\exp(-i\omega t)$. For waves of small amplitude, ϕ solves the following well-known, linear, two-dimensional boundary-value problem.

Scattering boundary-value problem $\mathscr{S}$

Determine the complex-valued total potential ϕ, such that ϕ satisfies Laplace's equation,

$$\left(\frac{\partial^2}{\partial x^2}+\frac{\partial^2}{\partial y^2}\right)\phi(x,y)=0 \quad \text{in the water}$$

the linearised free-surface condition

$$K\phi+\frac{\partial\phi}{\partial y}=0 \quad \text{on} \quad y=0,\ |x|>a \tag{2.1}$$

the boundary condition on the cylinder

$$\frac{\partial\phi}{\partial r}=0 \quad \text{on} \quad r=a,\ -\tfrac{1}{2}\pi\leqslant\theta\leqslant\tfrac{1}{2}\pi \tag{2.2}$$

and $\phi-\phi_I$ satisfies a 'radiation' condition, which ensures that $\phi-\phi_I$ represents outgoing waves at infinity. Here, $K=\omega^2/g$, where g is the acceleration due to gravity, (r,θ) are circular polar coordinates defined by

$$x=r\sin\theta, \quad y=r\cos\theta$$

and ϕ_I is the velocity potential of the incident wave, i.e.

$$\phi_I=\frac{Ag}{\omega}\exp(-Ky-iKx) \tag{2.3}$$

Since the downward surface elevation is given by

$$\eta(x)=-i\omega\phi(x,0)/g \tag{2.4}$$

we see that the incident wave has amplitude A.

Let us write the total velocity potential as

$$\phi=\phi_I+\phi_D \tag{2.5}$$

Then ϕ_D solves the

Diffraction boundary-value problem $\mathscr{D}$

Determine the complex-valued diffraction potential ϕ_D, such that ϕ_D satisfies Laplace's equation in the water, the free-surface condition (2.1), the boundary condition

$$\frac{\partial\phi_D}{\partial r}=-\frac{\partial\phi_I}{\partial r} \quad \text{on} \quad r=a,\ -\tfrac{1}{2}\pi\leqslant\theta\leqslant\tfrac{1}{2}\pi \tag{2.6}$$

and a radiation condition at infinity.

Thus, ϕ_D is a *radiation* potential, corresponding to a certain prescribed normal velocity on the cylinder. Moreover, the existence and uniqueness theorems of John[8] assure us that there is precisely one function ϕ_D that solves $\mathscr{D}$. We should remark that John's theorems are *not* applicable when the cylinder is partially immersed with a non-zero value of d. (If $-a<d<0$, John's results prove uniqueness, but not existence; if $0<d<a$, they prove neither.)

Several authors have studied the scattering problem $\mathscr{S}$. However, before reviewing their work, let us define the physical quantities of interest; these are also the quantities that may be determined by experiment.

The incident wave will be partially reflected and partially transmitted. Let $\eta\to\eta_\pm$ as $x\to\pm\infty$, where η is defined by equation (2.4). The *reflection coefficient* R, and the *transmission coefficient* T are defined by

$$\eta_+(x)=-iA[\exp(-iKx)+R\exp(iKx)] \tag{2.7}$$

and

$$\eta_-(x)=-iAT\exp(-iKx) \tag{2.8}$$

Since the surface elevation of the incident wave is

$$\eta_I(x)=-iA\exp(-iKx) \tag{2.9}$$

we see that

$$\eta_+=[1+R\exp(2iKx)]\,\eta_I$$

and

$$\eta_-=T\eta_I$$

R and T are related by

$$|R|^2 + |T|^2 = 1 \tag{2.10}$$

and

$$|\arg R - \arg T| = \tfrac{1}{2}\pi \text{ modulo } \pi \tag{2.11}$$

Equation (2.10) follows from a simple energy argument, whilst equation (2.11) has been derived by Newman.[9] Both of these relations may be used to check numerical calculations.

The incident wave will induce a dynamic force on the cylinder; this force has components X and Y (per unit length of the cylinder) in the x and y directions, respectively. X and Y are obtained by integrating the dynamic component of the pressure over the mean wetted surface of the cylinder. Thus:

$$X = -\rho i\omega a \int_{-\frac{1}{2}\pi}^{\frac{1}{2}\pi} \langle\phi\rangle \sin\theta \, d\theta \tag{2.12}$$

and

$$Y = -\rho i\omega a \int_{-\frac{1}{2}\pi}^{\frac{1}{2}\pi} \langle\phi\rangle \cos\theta \, d\theta \tag{2.13}$$

where we use angular brackets to indicate that r is to be put equal to a. We define dimensionless force coefficients, f_x and f_y, by

$$X = \rho g a A f_x \quad \text{and} \quad Y = \rho g a A f_y \tag{2.14}$$

The four complex quantities, R, T, f_x and f_y, are all functions of a single dimensionless variable, namely Ka; several authors have attempted to determine these functions. Dean and Ursell[3] have used Ursell's[10] 'multipole method', in which ϕ_D is represented as an infinite series of multipole potentials (see Section 3), i.e.

$$\phi_D(r,\theta) = \sum_{m=0}^{\infty} c_m \Phi_m(r,\theta) \tag{2.15}$$

(Φ_m are the known multipole potentials and the coefficients c_m are to be determined). Equation (2.15) satisfies all the conditions of problem $\mathscr{D}$, except the boundary condition equation (2.6); using this, we obtain:

$$\left\langle -\frac{\partial}{\partial r}\phi_I(\theta)\right\rangle = \sum_{m=0}^{\infty} c_m \left\langle \frac{\partial}{\partial r}\Phi_m(\theta)\right\rangle \quad -\tfrac{1}{2}\pi \leqslant \theta \leqslant \tfrac{1}{2}\pi \tag{2.16}$$

Essentially, Dean and Ursell multiplied equation (2.16) by each of a complete set of trigonometric functions and integrated over θ, yielding an infinite system of linear algebraic equations for the unknown coefficients c_m. By truncating this system, they were able to obtain numerical solutions; their results were presented as graphs of $|R|$, $|T|$, $|f_x|$ and $|f_y|$, against Ka.

Barakat[11] has also used the multipole method to solve $\mathscr{D}$, but used a least-squares technique to solve (2.16). He presented graphical results for the same quantities as Dean and Ursell, and also for cylinders of other cross-sections. In an earlier draft,[12] he described his technique in more detail, and also gave tables of values of $|T|$, $|f_x|$ and $|f_y|$, for several values of Ka; we shall examine these in Section 3.

Integral-equation methods have also been used to solve $\mathscr{D}$. Kim[13] represented ϕ_D by a distribution of wave sources over the mean wetted surface, and then determined the unknown source strength by solving an integral equation of the second kind (the source integral equation). He has computed dimensionless forms of $X - X_I$ and $Y - Y_I$, for several cylinders of elliptic cross-section, where X_I and Y_I are the components of the Froude-Krylov force. (By definition, $X = X_I$ and $Y = Y_I$ when $\phi = \phi_I$, i.e. when $\phi_D = 0$.) More recently, Naftzger and Chakrabarti[14] have solved $\mathscr{D}$ for water of constant finite depth, by solving Green's integral equation for $\langle\phi_D\rangle$. They have presented graphs of f_x, f_y and $|R|$, against Ka, for several depths of water.

All of the methods we have described so far yield (numerical) solutions for small, or moderate values of Ka; for large values of Ka, other methods must be employed. Ursell[15] has given a rigorous asymptotic solution of $\mathscr{P}$, by deriving a Fredholm integral equation of the second kind for $\langle\phi\rangle$, with a 'small' kernel. He solved this equation by iteration, and obtained the following asymptotic estimate for T:

$$T \sim (2i/\pi)(Ka)^{-4}\exp(-2iKa) \tag{2.17}$$

Leppington[16] has rederived this result, using matched asymptotic expansions; he has also obtained similar results for a half-immersed elliptic cylinder, and for a half-immersed circular cylinder with a vertical keel. Alker[17] has used similar methods to treat the problem of a partially immersed cylinder, with $-a < d \leqslant 0$.

We conclude this brief review by mentioning two pertinent review articles, by Newman[18] and Mei.[19] In the next section, we shall give a detailed description of the multipole method.

3. THE MULTIPOLE METHOD

The potential of the incident wave is given by (2.3) as

$$\phi_I = \phi_I^1 + \phi_I^2$$

where

$$\phi_I^1 = Ag\omega^{-1}\exp(-Ky)\cos Kx$$

and

$$\phi_I^2 = -iAg\omega^{-1}\exp(-Ky)\sin Kx \tag{3.1}$$

are even and odd, respectively, about $\theta = 0$. We decompose the diffraction potential in a similar manner, and represent each component by an infinite series of multipole potentials. Thus:

$$\phi_D = \phi_D^1 + \phi_D^2$$

where

$$\phi_D^1 = Ag\omega^{-1}\left\{c_1^1\Phi_0^1 + \sum_{m=1}^{\infty} a^{2m}c_{m+1}^1\Phi_m^1\right\}$$

and (3.2)

$$\phi_D^2 = Ag\omega^{-1}\left\{c_1^2\Phi_0^2 + \sum_{m=1}^{\infty} a^{2m+1}c_{m+1}^2\Phi_m^2\right\}$$

c_m^σ are coefficients to be determined, and Φ_m^σ are the multipole potentials, defined as follows:[20]

$$\Phi_0^1(r,\theta) = \int_0^{\infty} \exp(-ky)\cos kx \frac{dk}{k-K}$$
$$\sim \pi i \exp(-Ky \pm iKx) \quad \text{as} \quad x \to \pm\infty \tag{3.3}$$

(where the path of integration passes below the pole at $k = K$)

$$\Phi_0^2(r,\theta) = -\frac{1}{K}\frac{\partial}{\partial x}\Phi_0^1 \sim \pm\pi \exp(-Ky \pm iKx) \quad \text{as } x \to \pm\infty \tag{3.4}$$

$$\Phi_m^1(r,\theta) = \frac{\cos 2m\theta}{r^{2m}} + \frac{K}{2m-1}\frac{\cos(2m-1)\theta}{r^{2m-1}} \quad m > 0 \tag{3.5}$$

and

$$\Phi_m^2(r,\theta) = \frac{\sin(2m+1)\theta}{r^{2m+1}} + \frac{K}{2m}\frac{\sin 2m\theta}{r^{2m}} \quad m > 0 \tag{3.6}$$

Φ_0^1 and Φ_0^2 represent a wave source and a horizontal wave dipole, respectively, situated at the origin. Similarly, Φ_m^1 and Φ_m^2 are even and odd wavefree potentials. Each Φ_m^σ satisfies Laplace's equation in the water, and the free-surface and radiation conditions.

The set $\{\Phi_m^\sigma\}$ is known to be complete for solutions of problem $\mathscr{D}$, and so we are permitted to use the representations in equation (3.2). Moreover, these representations satisfy all the conditions of problem $\mathscr{D}$, except the boundary condition on the cylinder. Using this, we obtain:

$$\left\langle a\frac{\partial}{\partial r}[-\exp(-Ky)\cos Kx]\right\rangle = c_1^1\left\langle a\frac{\partial}{\partial r}\Phi_0^1\right\rangle + \sum_{n,1=1}^{\infty} c_{m+1}^1\left\langle a^{2m+1}\frac{\partial}{\partial r}\Phi_m^1\right\rangle \tag{3.7}$$

$$\left\langle a\frac{\partial}{\partial r}[i\exp(-Ky)\sin Kx]\right\rangle = c_1^2\left\langle a\frac{\partial}{\partial r}\Phi_0^2\right\rangle + \sum_{m=1}^{\infty} c_{m+1}^2\left\langle a^{2m+2}\frac{\partial}{\partial r}\Phi_m^2\right\rangle \tag{3.8}$$

These two equations are to be satisfied for $0 \leqslant \theta \leqslant \frac{1}{2}\pi$. In order to solve them, we multiply equations (3.7) and (3.8) by $\cos 2n\theta$ and $\sin(2n+1)\theta$, respectively, and then integrate over θ. We obtain the following two uncoupled infinite systems of complex, linear, algebraic equations for the unknown coefficients c_m^σ ($\sigma = 1, 2$):

$$\sum_{m=1}^{\infty} A_{nm}^\sigma c_m^\sigma = b_n^\sigma \qquad n = 1, 2, \ldots \tag{3.9}$$

A_{nm}^σ and b_n^σ may be evaluated explicitly; expressions for these are given in Appendix A.

Once the c_m^σ have been determined, we can evaluate R, T, f_x and f_y. From the definitions of R and T, and the behaviour of Φ_0^σ at large distances (given by equations (3.3) and (3.4)), we find that

$$R = \pi(ic_1^1 + c_1^2)$$

and

$$T = 1 + \pi(ic_1^1 - c_1^2)$$

Expressions for f_x and f_y, in terms of c_m^σ may also be obtained; these are also given in Appendix A.

Table 2. Theoretical values for f_x and f_y

Ka	$\lvert f_x\rvert$	$\arg f_x$	$\lvert f_y\rvert$	$\arg f_y$
0.01	3.143 (−2)	−3.1413	1.933	−1.5901
0.02	6.290 (−2)	−3.1404	1.886	−1.6085
0.03	9.444 (−2)	−3.1388	1.846	−1.6262
0.04	1.261 (−1)	−3.1367	1.811	−1.6433
0.05	1.578 (−1)	−3.1340	1.779	−1.6600
0.06	1.895 (−1)	−3.1308	1.750	−1.6761
0.07	2.214 (−1)	−3.1270	1.723	−1.6919
0.08	2.532 (−1)	−3.1227	1.697	−1.7073
0.09	2.851 (−1)	−3.1179	1.674	−1.7224
0.1	3.170 (−1)	−3.1125	1.651	−1.7372
0.2	6.269 (−1)	−3.0366	1.470	−1.8728
0.3	8.879 (−1)	−2.9386	1.335	−1.9936
0.4	1.065	−2.8479	1.224	−2.1055
0.5	1.156	−2.7847	1.129	−2.2118
0.6	1.186	−2.7548	1.046	−2.3144
0.7	1.180	−2.7547	9.714 (−1)	−2.4145
0.8	1.154	−2.7781	9.046 (−1)	−2.5129
0.9	1.121	−2.8191	8.441 (−1)	−2.6103
1.0	1.083	−2.8732	7.890 (−1)	−2.7069
2.0	7.769 (−1)	2.5879	4.355 (−1)	2.6145
3.0	5.972 (−1)	1.6330	2.691 (−1)	1.6401
4.0	4.815 (−1)	0.6533	1.802 (−1)	0.6559
5.0	4.012 (−1)	−0.3350	1.280 (−1)	−0.3339
6.0	3.425 (−1)	−1.3272	9.506 (−2)	−1.3267
7.0	2.980 (−1)	−2.3217	7.310 (−2)	−2.3214
8.0	2.632 (−1)	2.9656	5.780 (−2)	2.9658
9.0	2.354 (−1)	1.9688	4.675 (−2)	1.9690
10.0	2.126 (−1)	0.9714	3.853 (−2)	0.9715

For numerical work, we must truncate the two infinite systems (3.9) ($\sigma = 1$ and $\sigma = 2$); for each σ, we solve the first N equations for the first N coefficients, c_m^σ. We have two checks on numerical convergence, both of which were used: we can test how well the two relations (2.10) and (2.11) are satisfied; and we can compare results at different values of N.

In Tables 1 and 2, we present our computed values of R, T, f_x and f_y, for $Ka = 0.01(0.01)0.1(0.1)1.0(1.0)10.0$. We prefer to present our results as tables of numbers, rather than graphs, since numerical values are (i) not generally available, and (ii), more useful when alternative computer programs (based on different mathematical methods) are to be evaluated. (Note that we give arguments of complex numbers in the range $(-\pi, \pi)$.)

By examining our computations, we have found that, for $Ka \leqslant 2$, we can evaluate the four complex quantities R, T, f_x and f_y, to at least four significant figures, by taking $N = 20$. As Ka was increased, we had to increase N in order to obtain the same accuracy. Thus, for $Ka \leqslant 15$, we can compute f_x and f_y to at least four significant figures with $N = 60$. This value of N is also sufficient to compute $\arg R$ and $\arg T$ to the same accuracy. For $Ka \geqslant 2.8$ (approximately), $|R| = 1.0$ to four significant figures. However, as Ka increases, it becomes more difficult to calculate $|T|$, using the multipole method. In Table 3, we give the computed values of T for $Ka = 10$, and several values of N. We see that at $N = 20$, 30 and 60, we have computed $|T|$ with an accuracy of zero, one and two significant figures, respectively. Moreover, Ursell's asymptotic formula, equation (2.17), gives $|T| = 0.000064$, i.e. at $Ka = 10$, the computed result and the asymptotic result differ by about 15%; at $Ka = 15$, they differ by about 7%.

Dean and Ursell[3] used essentially the method described above. They made their calculations for 16 values of Ka in the range $0.01 < Ka < 10$, and with $N = 11$; curves of $|f_x|$,

Table 3. Numerical convergence of T at Ka = 10

N	$\lvert T\rvert \times 10^5$	arg T
20	3.357	0.37097
30	6.522	0.37179
40	7.136	0.37201
50	7.310	0.37209
60	7.374	0.37213
70	7.402	0.37215
80	7.415	0.37216
90	7.422	0.37216
100	7.426	0.37217
110	7.428	0.37217

Table 4. Numerical results of Barakat and Houston[12]

Ka	$\lvert T\rvert$	$\lvert f_x\rvert$	$\lvert f_y\rvert$
0.1	–	0.3171	1.6511
0.2	0.9185	–	–
0.4	0.6763	–	–
0.6	0.4263	–	–
0.8	0.2619	–	0.9108
1.0	0.1653	1.0956	–
2.0	0.0269	0.7903	–
3.0	0.0077	–	0.2691
4.0	0.0033	0.4704	–
5.0	0.0018	–	–
6.0	0.0012	0.3212	0.0936

$|f_y|$, $|R|$ and $|T|$ were drawn; these are probably sufficiently accurate for comparisons with their experiments (see Section 5).

Barakat and Houston[12] have solved equations (3.7) and (3.8) by a different method. Consider equation (3.7), which must hold for $0 \leqslant \theta \leqslant \frac{1}{2}\pi$. They replaced the infinite series by its first six terms (i.e. $N = 7$), and then evaluated the resulting equation at $\theta = 0°(4.5°)90°$, yielding 21 equations for the seven unknowns, $c_1^1, c_2^1, \ldots, c_7^1$; they solved these by a least-squares technique. In Table 4, we reproduce their results for $|T|$, $|f_x|$ and $|f_y|$; these may be compared with Tables 1 and 2; for some quantities (e.g. $|f_y|$ at $Ka = 3$), we find complete agreement, but for others (e.g. $|T|$ at $Ka = 4$), we find no significant figures in agreement.

4. EXPERIMENTAL INVESTIGATION

In order to test the validity of linearised potential theory (as presented in Section 2), experiments have been performed. The measurements were made in the narrow wave tank at the Department of Mechanical Engineering, University of Edinburgh, using facilities developed as part of the Edinburgh Wave Power Project.

The wave tank is 10 m long, 30 cm wide, and holds water to a depth of 60 cm. At one end of the tank, there is an *absorbing*, hinged-plate wave-maker; by varying the electronic drive to the wave-maker, regular waves of a given frequency are generated, even when waves (produced by reflection at a cylinder, say) are incident upon the wave-maker. At the other end of the tank, there is an absorbing beach. This consists of a vertical wedge of 'Expamet', packed into a cage, with the density increasing towards the rear. (Expamet, which is designed for use as a filter material, is made from thin sheets of metal, with a pattern of slits which is pulled out and corrugated.) Reflections from the beach amount to less than 5%.

Wave amplitude was measured with a float gauge. This consists of a cylindrical float (made of expanded polystyrene) which stretches across the entire width of the tank and which is constrained to move vertically by a linkage at each end. (Since all wave tanks are prone to sideways oscillations, it is important that the *average* wave height is measured.) The linkage is attached to the movement of a microammeter, resulting in a signal which is proportional to the velocity of the float. Some analogue electronic computation then yields the wave amplitude (after calibration).

A single wave gauge of his type cannot determine in which direction a wave is travelling; thus, it cannot distinguish between an incident wave and a reflected wave. However, this difficulty can be overcome by using two wave gauges. The procedure is to place the two gauges one-quarter of a wavelength apart, and then to search along the tank for a position where the difference between the two signals is maximised. The amplitude of the reflected wave is then half this difference, and the amplitude of the incident wave is the average of the two signals; see Appendix B for a proof of these statements.

The cylinder used was neutrally buoyant, and made of a light alloy; its radius and length were $a = 5$ cm and $l = 29.5$ cm, respectively. Vertically above the cylinder axis, there were two force transducers, which responded only to horizontal forces on the cylinder. To the left of these transducers, there was another pair which responded to both horizontal and vertical forces. (The transducers consisted of strain gauges on thin-walled phosphor bronze torque tubes.) Some analogue electronic computation yielded the two forces separately (after static calibration using weights). (A photograph of the cylinder mounting and force measuring rig is given on p. 431 of reference 5.)

Three series of experiments were performed:

Series 1. Variation of exciting forces with amplitude of incident wave; frequency fixed. Mean horizontal forces were also measured.

Series 2. Variation of exciting forces with frequency; amplitude of incident wave fixed.

Series 3. Variation of reflection coefficient with amplitude of incident wave; frequency fixed. We remark that this series has been repeated by Dixon[21] for 13 other values of $d(-0.8 \leqslant (d/a) \leqslant 1.8)$; however, there is no relevant theory with which to compare his measurements.

For any given frequency, the wavenumber K is determined numerically from the dispersion relation:

$$\omega^2 = gK \tanh Kh \tag{4.1}$$

where h is the depth of water ($h = 0.6$ m) and $g = 9.815$ m s^{-2} ($f = \omega/2\pi$ is the frequency in Hz).

When measuring forces, three numbers were recorded: the maximum positive force during one cycle (F^+); the minimum negative force during one cycle (F^-); and the root-mean-square force (F^{rms}). (For a given force $F(t)$, its rms value is given by:

$$(F^{\text{rms}})^2 = \frac{1}{T}\int_0^T \{F(t)\}^2 \, dt$$

where $T = 2\pi/\omega$ is the period.) From these three numbers, the amplitude of the experimental force is calculated in two ways:

$$F^1 = \tfrac{1}{2}|F^+ - F^-| \quad \text{and} \quad F^2 = 2^{1/2}F^{\text{rms}}$$

If $F(t) = \mathrm{Re}\{\mathscr{F}\exp(-i\omega t)\}$, for some complex number $\mathscr{F}$, then $F^1 = F^2 = |\mathscr{F}|$. In practice, the two measures are different. F^1, which is simply one half of the peak-to-trough height, is the measure that was used by Dean and Ursell[3] in their experiments. Dimensionless quantities f^1 and f^2 are obtained from F^1 and F^2, respectively, by dividing by $\rho g a A l (\rho = 10^3\ \mathrm{kg\ m^{-3}})$. Note that a subscript x will be added to denote various horizontal forces, and similarly with a subscript y for vertical forces.

The results from each series of experiments are presented in the next section, together with a comparison with the linear theory of Section 2.

5. COMPARISON OF THEORY AND EXPERIMENT

The experiments were performed at several of the frequencies (f) listed in Table 5. This table also includes the theoretical values of Ka, L (the wavelength), $|f_x|$, $|f_y|$ and $|R|$. (In this section, we shall write R for $|R|$, etc, since we shall only be comparing magnitudes.) Note that these last three quantities are independent of A, the amplitude of the incident wave.

Series 1. The results for this series are presented in Tables 6 and 7. All these experiments were conducted at the same frequency, namely 1.0 Hz ($\omega = 2\pi$); the corresponding theoretical values for f_x and f_y are 0.639 and 1.463, respectively.

A comparison between theory and experiment is given in Fig. 1. We see that the linear theory predicts the horizontal forces very accurately; even at $A/a = 0.6$, f_x and f_x^2 differ by less than 3%; note, also, that $|f_x - f_x^2|$ is consistently smaller than $|f_x - f_x^1|$. However, the vertical forces are predicted rather less accurately; at $A/a = 0.2$, f_y and f_y^2 differ by about 5%; at $A/a = 0.4$, they differ by about 8%. Dean and Ursell[3] obtained better agreement (see Fig. 3), but they used much smaller values of A/a in their experiments ($0.01 \leqslant (A/a) \leqslant 0.18$). We conclude that linear theory gives an accurate prediction of vertical forces when A/a is sufficiently small.

Series 2. The results for this series are presented in Tables 8 and 9 (the theoretical values are given in Table 5). In all these experiments, the value of A/a was 0.4. In Fig. 2, we give a comparison between the theoretical and experimental values of f_x. The experimental data of Dean

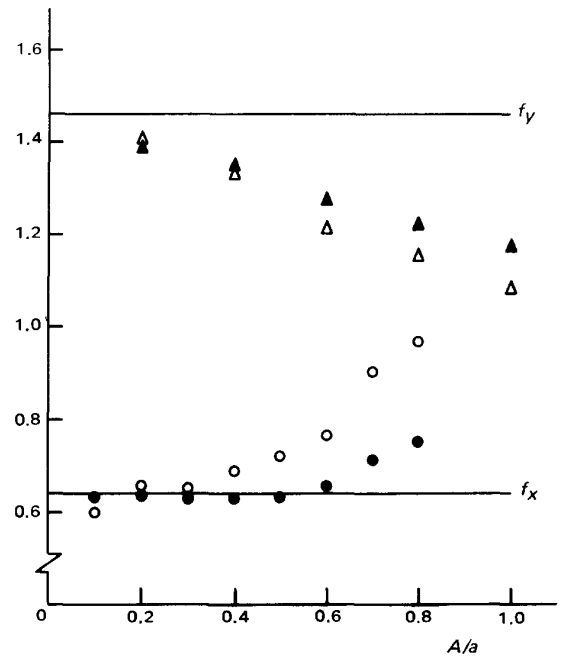

Figure 1. Comparison of theoretical and experimental values of f_x and f_y; $f = 1.0$ Hz. The theoretical values (shown as solid lines) are independent of A/a. ○, f_x^1; ●, f_x^2; △, f_y^1; ▲, f_y^2

Table 5. Theoretical values for comparison with experiment

f (Hz)	Ka	L (m)	$\lvert f_x\rvert$	$\lvert f_y\rvert$	$\lvert R\rvert$
0.6	0.0908	3.458	0.288	1.672	–
0.75	0.1250	2.514	–	–	0.244
0.80	0.1384	2.271	0.439	1.573	–
1.00	0.2041	1.539	0.639	1.463	0.404
1.20	0.2902	1.083	0.866	1.347	–
1.25	0.3146	0.999	–	–	0.611
1.40	0.3942	0.797	1.057	1.230	–

Table 6. Measured values of horizontal forces; $f = 1.0$ Hz; theoretical value, $f_x = 0.639$, independent of A/a

A/a	$F_x^+(N)$	$F_x^-(N)$	$F_x^{\mathrm{rms}}(N)$	f_x^1	f_x^2
0.1	0.586	−0.293	0.324	0.607	0.633
0.2	1.172	−0.732	0.647	0.658	0.632
0.3	1.660	−1.172	0.958	0.652	0.624
0.4	2.344	−1.660	1.286	0.691	0.628
0.5	2.881	−2.344	1.621	0.722	0.633
0.6	3.467	−3.174	2.019	0.765	0.657
0.7	4.736	−4.443	2.550	0.906	0.712
0.8	5.566	−5.664	3.079	0.970	0.752

Table 7. As for Table 6, but for vertical forces; theoretical value, $f_y = 1.463$

A/a	$F_y^+(N)$	$F_y^-(N)$	$F_y^{\mathrm{rms}}(N)$	f_y^1	f_y^2
0.2	2.129	−1.934	1.422	1.403	1.389
0.4	4.390	−3.330	2.758	1.333	1.347
0.6	6.367	−4.175	3.908	1.214	1.273
0.8	8.643	−4.775	5.021	1.159	1.226
1.0	9.995	−5.703	6.015	1.084	1.175

Table 8. Measured values of horizontal forces; $A/a = 0.4$

f (Hz)	$F_x^+(N)$	$F_x^-(N)$	$F_x^{\mathrm{rms}}(N)$	f_x^1	f_x^2
0.6	1.270	−0.830	0.663	0.363	0.324
0.8	2.148	−1.514	1.071	0.632	0.523
1.0	2.344	−1.660	1.286	0.691	0.628
1.2	2.930	−2.344	1.683	0.911	0.822
1.4	2.832	−2.686	1.830	0.953	0.894

Table 9. As for Table 8, but for vertical forces

f (Hz)	$F_y^+(N)$	$F_y^-(N)$	$F_y^{\mathrm{rms}}(N)$	f_y^1	f_y^2
0.6	4.932	−4.351	3.341	1.603	1.632
0.8	4.702	−4.106	3.158	1.521	1.542
1.0	4.390	−3.330	2.758	1.333	1.347
1.2	3.882	−2.744	2.431	1.144	1.187
1.4	3.296	−2.148	2.059	0.940	1.006

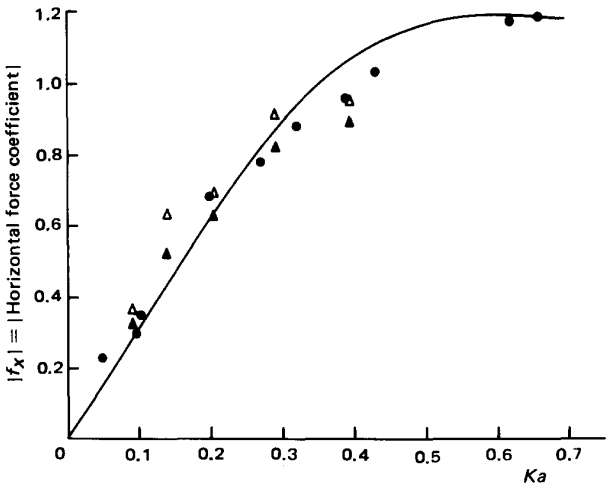

Figure 2. Comparison of theoretical and experimental values of f_x; $A/a = 0.4$. ●, Dean and Ursell; △, f_x^1; ▲, f_x^2; theory, ——

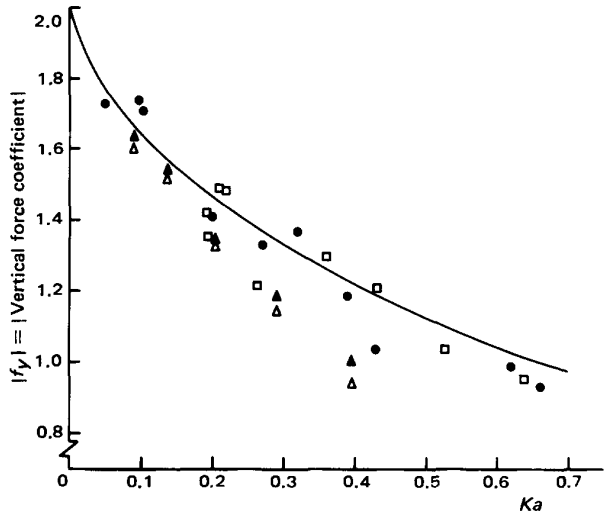

Figure 3. Comparison of theoretical and experimental values of f_y; $A/a = 0.4$. ●, Dean and Ursell; □, Yu and Ursell; △, f_y^1; ▲, f_y^2; theory, ——

and Ursell are also included. The agreement is seen to be good, at all the frequencies considered.

In Fig. 3, we give a similar comparison for f_y; again, we include Dean and Ursell's data. The difference between our data points and the theoretical curve is seen to increase as Ka increases. This is not true of Dean and Ursell's data. Moreover, it cannot be due to the finite depth of water, for such effects become *smaller* as Ka increases (i.e. as the wavelength shortens). We believe that the differences are due to the rather large value of A/a used, namely 0.4, because (i) we showed in Series 1 (see Fig. 1) that significant differences occur at such values of A/a, and (ii), Dean and Ursell obtained better agreement using smaller values of A/a (maximum value, 0.18).

Yu and Ursell[22] have performed a related series of experiments: they measured the amplitude ratio R_A, for a half-immersed circular cylinder which is forced to make small simple-harmonic oscillations in the vertical direction. (R_A is the amplitude of the radiated waves, at large distances from the cylinder, when the cylinder makes forced oscillations of unit amplitude.) We may use one of the Haskind relations (see, e.g., Newman[23]) to determine f_y from R_A:

$$f_y = R_A D/(Ka) \tag{5.1}$$

where K is the solution of equation (4.1) and

$$D = \tanh Kh + Kh\,\mathrm{sech}^2 Kh \tag{5.2}$$

($D \to 1$ as $h \to \infty$). We have taken Yu and Ursell's data for $a/h = 0.13$ (their Table 1), and computed f_y from equation (5.1); the results are given in Table 10 (for $Ka < 1.0$) and are also plotted in Fig. 3. Again, the agreement with linear theory is satisfactory; the usefulness of the Haskind relation has also been demonstrated.

Series 3. The reflection coefficient R was measured for seven values of A/a and three frequencies; the results are presented in Table 11, and plotted with the theoretical

Table 10. Experimental data of Yu and Ursell; $a/h = 0.13$; $2\pi/L_\infty = \omega^2/g$. f_y is determined from R_A, using a Haskind relation

L_∞(ft)	Ka	R_A	D	f_y
9.10	0.1924	0.231	1.182	1.419
9.00	0.1940	0.223	1.180	1.357
8.20	0.2085	0.267	1.166	1.493
7.61	0.2213	0.286	1.151	1.488
6.20	0.2629	0.289	1.106	1.216
4.40	0.3600	0.451	1.036	1.298
3.65	0.4316	0.514	1.017	1.211
2.98	0.5275	0.543	1.007	1.037
2.46	0.6386	0.610	1.000	0.955
1.87	0.8400	0.695	1.000	0.827
1.67	0.9406	0.735	1.000	0.781

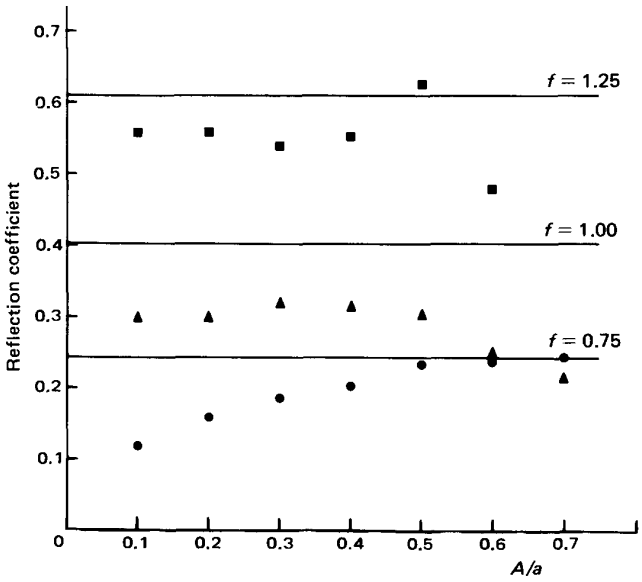

Figure 4. Comparison of theoretical and experimental values of $|R|$, at three frequencies. Solid lines are theoretical values (independent of A/a). ●, $f = 0.75$ Hz; ▲, $f = 1.00$ Hz; ■, $f = 1.25$ Hz

values (see Table 5) in Fig. 4. We see that R is almost independent of A/a; for $f = 0.75$ Hz, R increases slowly with A/a. However, the agreement with linear theory is poor; the measured values are nearly all less than the theoretical values; at $A/a = 0.1$ (where we expect the best agreement), the differences between theory and experiment are about 8.3% ($f = 1.25$), 26% ($f = 1.0$) and 51% ($f = 0.75$). For the lower frequencies, finite-depth effects are probably important. (The conventional deep-water limit is $h/L > 0.5$, which is only satisfied here when $f = 1.25$; however, this limit may not be applicable when an immersed body is present.) However, these do not account for the significant difference at $f = 1.25$ Hz.

Dean and Ursell[3] have measured R for a range of frequencies. They found that the average difference between theory and experiment was about 14%, and that the measured values were always less than the theoretical values. This is in broad agreement with our findings. Dean and Ursell also measured T; they found very good agreement with theory (average algebraic difference = 0.2%). Using their measured values of R and T, they checked how well the energy relation (2.10) was satisfied. They found an average energy loss of about 10%, apparently occurring mainly in the reflected component (because of the good agreement between the theoretical and measured values of T). In order to account for this loss of energy, Dean and Ursell made some simple calculations; after showing that viscous effects and surface-tension effects were both negligible, they suggested the following two mechanisms:

(i) Higher harmonics in the wave motion generated by the wave-maker.

(ii) Possibility of vorticity in the reflection process.

With regard to (i), they estimated that, for their wave-maker, the amplitude of the higher harmonics was about 5% of the amplitude of the fundamental wave. Our wave-maker has been shown to produce waves of a similar quality (see p. 18.2 of Jeffrey *et al.*[4]), and so we cannot rule out this mechanism. We are also unable to rule out the second mechanism, since our theory assumes that the fluid motion is irrotational.

Mean horizontal forces. Let us conclude this section by examining the mean horizontal forces ('drift' forces) on the cylinder. Such forces cannot be predicted by the first-order linear theory (where all quantities are time-harmonic with frequency $f = \omega/2\pi$); they are a second-order effect, as are forces with frequency $2f$. (For a recent discussion of drift forces on immersed bodies, see Chakrabarti.[24]) Instead of developing a second-order theory, we shall use a simple formula, involving only first-order quantities, which was obtained by Longuet-Higgins.[7] He used simple arguments, based on the conservation of mean momentum, to show that the mean horizontal force, per unit length of the cylinder, is given by:

$$F \simeq -\tfrac{1}{4}\rho g A^2 D'(1 + |R|^2 - |T|^2)$$

in the positive x-direction, where $D' = D/\tanh Kh$ and D is defined by equation (5.2). As before, we divide by $\rho g a A$ and define a corresponding dimensionless force coefficient, f_m, by:

$$f_m = -\tfrac{1}{4}(1 + |R|^2 - |T|^2)\, D'A/a \qquad (5.3)$$

If the energy relation (2.10) is satisfied, equation (5.3) becomes:

$$f_m = -\tfrac{1}{2}|R|^2 D'A/a \qquad (5.4)$$

Table 11. Measured values of $|R|$

	Frequency, f (Hz)		
A/a	0.75	1.00	1.25
0.1	0.120	0.300	0.560
0.2	0.160	0.300	0.560
0.3	0.187	0.320	0.540
0.4	0.205	0.315	0.555
0.5	0.236	0.304	0.628
0.6	0.237	0.250	0.480
0.7	0.243	0.214	-*

* Unstable sideways oscillations in tank

Table 12. Measured values of the mean horizontal force; $f = 1.0$ Hz; $f_m = F/(\rho g a A l)$

A/a	F(N)	f_m	f_m^1	f_m^2
0.1	0.120	0.166	−0.009	−0.007
0.2	0.114	0.079	−0.018	−0.014
0.3	0.101	0.047	−0.026	−0.021
0.4	0.060	0.021	−0.035	−0.028
0.5	0.000	0.000	−0.044	−0.034
0.6	−0.062	−0.014	−0.053	−0.036
0.7	−0.167	−0.033	−0.061	−0.039
0.8	−0.257	−0.044	−0.070	–

We have measured the mean horizontal force for various values of A/a, and $f = 1.0$ Hz; the results, and the corresponding values of f_m are given in Table 12. We can compare these results with two formulae:

(i) Assume that the energy relation is satisfied and use the theoretical value of R (= 0.404); equation (5.4) becomes ($D' = 1.073$)

$$f_m^1 = -0.088 A/a$$

(ii) Use equation (5.3) with the theoretical value of T (= 0.915) and the measured values of R (see Table 11; measured values of T are not available), i.e.:

$$f_m^2 = -0.268(R^2 + 0.163)\, A/a$$

The corresponding results are also given in Table 12, and a comparison is shown in Fig. 5. Both formulae predict that f_m is negative, i.e. that the mean force and the incident wavetrain are always in the same direction. This is not borne out by experiment. Indeed, the smallest waves produced the largest positive forces. Longuet-Higgins[7] has suggested that this phenomenon may be partly due to the generation of second harmonics in the transmitted wave.

6. CONCLUSIONS

In this paper, we have studied a canonical water-wave scattering problem, namely, the interaction of a train of regular surface waves with a fixed, half-immersed circular cylinder. We have studied this problem theoretically and experimentally, and compared results from each approach

We began by formulating the well-known two-dimensional linear boundary-value problems of classical hydrodynamics. We used the multipole method to solve the diffraction problem, $\mathscr{D}$; accurate numerical solutions have been obtained. In particular, we have given tables of four important (complex) quantities (for $0.01 \leqslant Ka \leqslant 10$); these are the reflection coefficient R, the transmission coefficient T, and the two force coefficients, f_x and f_y.

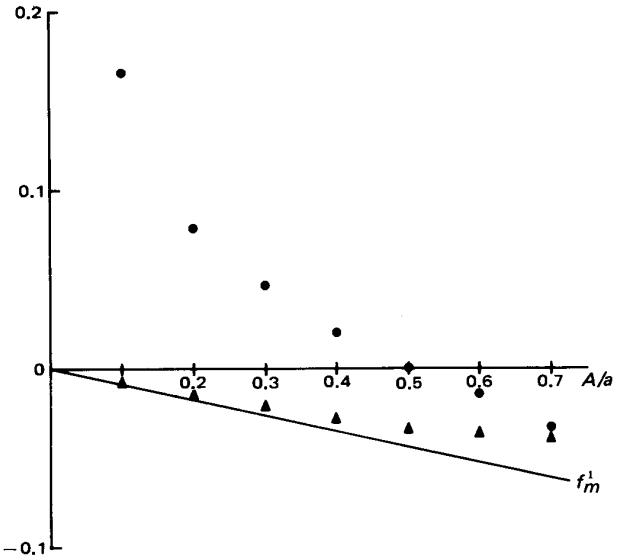

Figure 5. Comparison of theoretical and experimental values of mean horizontal force; $f = 1.0$ Hz; ●, experiment; f_m^1, ——; f_m^2, ——▲

Numerically, the multipole method is inefficient at large values of Ka; in particular, the computation of $|T|$ was shown to be especially difficult (see Table 3). We have attempted to show that our numerical solution for $|T|$ is in agreement with Ursell's[15] asymptotic solution; at $Ka = 15$, the difference between the two is about 7%. A better method for showing such agreement might be to solve Ursell's integral equation, numerically, at moderate values of Ka; to the authors' knowledge, nobody has tried to do this.

Experiments have been performed to measure the forces on a half-immersed cylinder, and also the reflection coefficient. We compared our results for $|f_x|$, $|f_y|$ and $|R|$ with those predicted by the linear theory. No measurements of phase were taken. We obtained the following results:

(1) The horizontal force coefficient, $|f_x|$, was predicted very accurately by the linear theory, even for quite large waves (at $A = 0.6a$, the error was less than 3%).

(2) The vertical force coefficient, $|f_y|$, was only predicted accurately for rather small amplitude waves ($A < 0.2a$). For a fixed amplitude ($A = 0.4a$), we found that the discrepancy between the measured and theoretical values increased as the frequency increased; this was attributed to the large value of A/a used in our experiments. We also used some data obtained by Yu and Ursell[22] (for the forced-heaving problem), together with a Haskind relation, in order to predict $|f_y|$; good agreement was found with the theory.

(3) The reflection coefficient, $|R|$, was not predicted accurately by the linear theory; even for small amplitude waves, the discrepancy was significant. At low frequencies, finite-depth effects are believed to be important; a more detailed numerical solution of this problem is required. However, at higher frequencies, finite-depth effects are small, but the difference between theory and experiment is not. The same phenomenon had previously been noted by Dean and Ursell.[3] They also measured $|T|$, and hence showed that energy is lost in the reflection process; the cause of this loss has yet to be established.

Finally we have also measured the mean horizontal forces on the cylinder; these are steady forces which are not predicted by the first-order linear theory. Rather than develop a second-order theory, we compared our measurements with a simple formula obtained by Longuet-Higgins.[7] Unfortunately, the agreement between this formula and our experiments is poor.

ACKNOWLEDGEMENTS

The authors would like to thank Mr Stephen Salter and his associates working on the Edinburgh Wave Power Project for making available their experimental facilities, and for much guidance and help in the data-collection process. The experimental program was carried out under the supervision of Dr C. A. Greated of the Department of Physics, University of Edinburgh. Thanks are also due to the Science Research Council for their financial support.

REFERENCES

1 Shaw, T. L. (ed.) *Mechanics of wave-induced forces on cylinders*, Pitman, London, 1979.
2 Hogben, N. *Fluid loading of offshore structures, a state of art appraisal: wave loads*, Royal Inst. Naval Arch., 1974
3 Dean, R. G. and Ursell, F. Interaction of a fixed, semi-immersed circular cylinder with a train of surface waves, *Tech. Rep. No. 36*, Hydro. Lab., Massachusetts Inst. of Tech., 1959
4 Jeffrey, D. C., Richmond, D. J. E., Salter, S. H. and Taylor, J. R. M. *2nd Year Interim Rep. on Edinburgh Wave Power Project*, Dept. of Mech. Eng., Univ. of Edinburgh, 1976
5 Dixon, A. G., Greated, C. A. and Salter, S. H. Wave forces on partially submerged cylinders, *J. Wat., Port, Coast. and Ocean Div., ASCE* 1979, **104**, 421
6 Hogben, N., Miller, B. L., Searle, J. W. and Ward, G. Estimation of fluid loading on offshore structures, *Proc. Inst. Civ. Eng., Part 2* 1977, **63**, 515
7 Longuet-Higgins, M. S. The mean forces exerted by waves on floating or submerged bodies with applications to sand bars and wave power machines, *Proc. Roy. Soc. A* 1977, **352**, 463
8 John, F. On the motion of floating bodies II, *Comm. Pure Appl. Math.* 1950, **3**, 45.
9 Newman, J. N. Propagation of water waves past long two-dimensional obstacles, *J. Fluid Mech.* 1965, **23**, 23
10 Ursell, F. On the heaving motion of a circular cylinder on the surface of a fluid, *Quart. J. Mech. Appl. Math.* 1949, **2**, 218
11 Barakat, R. The interaction of surface waves with fixed semi-immersed cylinders having symmetric cross-sections, *Appl. Sci. Res.* 1970, **22**, 1
12 Barakat, R. and Houston, A. The interaction of surface waves with a fixed cylinder lying in the free surface, Tech. Rep., Optics Dept., Itek Corp., Lexington, Massachusetts, undated
13 Kim, W. D. On the surging, heaving and rolling motions of floating cylinders, Tech. Rep., Boeing Sci. Res. Labs., Seattle, Washington, 1964
14 Naftzger, R. A. and Chakrabarti, S. K. Scattering of waves by two-dimensional circular obstacles in finite water depths, *J. Ship Res.* 1979, **23**, 32
15 Ursell, F. The transmission of surface waves under surface obstacles, *Proc. Cambridge Phil. Soc.* 1961, **57**, 638
16 Leppington, F. G. On the radiation and scattering of short surface waves, Part 2, *J. Fluid Mech.* 1973, **59**, 129
17 Alker, G. The scattering of short waves by a cylinder, *J. Fluid Mech.* 1977, **82**, 673
18 Newman, J. N. Diffraction of water waves, *Appl. Mech. Rev.* 1972, **25**, 1
19 Mei, C. C. Numerical methods in water-wave diffraction and radiation, *Ann. Rev. Fluid Mech.* 1978, **10**, 393
20 Thorne, R. C. Multipole expansions in the theory of surface waves, *Proc. Cambridge Phil. Soc.* 1953, **49**, 707
21 Dixon, A. G. Wave forces on cylinders, *PhD thesis*, Univ. of Edinburgh, 1980
22 Yu. Y. S. and Ursell, F. Surface waves generated by an oscillating circular cylinder on water of finite depth: theory and experiment, *J. Fluid Mech.* 1961, **11**, 529

23 Newman, J. N. The interaction of stationary vessels with regular waves, *Proc. 11th Symp. Naval Hydrodynamics*, London, 1976, 491-501

24 Chakrabarti, S. K. Steady and oscillating drift forces on floating objects, *J. Wat., Port, Coast. and Ocean Div., ASCE* 1980, **106**, 205

APPENDIX A

The wave source Φ_0^1 may be evaluated using the power-series expansion[22]

$$\Phi_0^1(Kr,\theta) = -(\log Kr - i\pi + \gamma)\sum_{m=0}^{\infty}\frac{(-Kr)^m}{m!}\cos m\theta + \theta\sum_{m=1}^{\infty}\frac{(-Kr)^m}{m!}\sin m\theta + \sum_{m=1}^{\infty}\frac{(-Kr)^m}{m!}\left(\frac{1}{1}+\frac{1}{2}+\ldots+\frac{1}{m}\right)\cos m\theta$$

where γ is Euler's constant ($\gamma = 0.5772\ldots$). Differentiating, we obtain

$$\Phi_0^2(Kr,\theta) = \frac{\sin\theta}{Kr} + (\log Kr - i\pi + \gamma)\sum_{m=1}^{\infty}\frac{(-Kr)^m}{m!}\sin m\theta + \theta\sum_{m=0}^{\infty}\frac{(-Kr)^m}{m!}\cos m\theta - \sum_{m=1}^{\infty}\frac{(-Kr)^m}{m!}\left(\frac{1}{1}+\frac{1}{2}+\ldots+\frac{1}{m}\right)\sin m\theta$$

Similar expansions may be obtained for $\partial\Phi_0^\sigma/\partial r$.

The matrix elements A_{nm}^σ and b_n^σ in equation (3.9) all involve elementary integrations over θ. Thus, for $n \geqslant 1$, $m \geqslant 2$

$$A_{n/m}^1 = \int_0^{\frac{1}{2}\pi}\left\langle a^{2m-1}\frac{\partial}{\partial r}\Phi_{m-1}^1\right\rangle \cos 2(n-1)\theta\ \mathrm{d}\theta$$

and

$$A_{nm}^2 = \int_0^{\frac{1}{2}\pi}\left\langle a^{2m}\frac{\partial}{\partial r}\Phi_{m-1}^2\right\rangle \sin(2n-1)\theta\ \mathrm{d}\theta$$

$$A_{nm}^\sigma = -\tfrac{1}{4}\pi p\delta_{nm} - Kaq(-1)^{m+n}/(p^2-q^2)$$

where $p = 2n-3+\sigma$, $q = 2m-4+\sigma$, and δ_{nm} is the Kronecker delta. Similarly

$$A_{11}^1 = \int_0^{\frac{1}{2}\pi}\left\langle a\frac{\partial}{\partial r}\Phi_0^1\right\rangle \mathrm{d}\theta = -\tfrac{1}{2}\pi\cos Ka + \sum_{j=0}^{\infty}\frac{(-1)^j(Ka)^{2j+1}}{(2j+1)!}G_{2j+1}$$

$$A_{n1}^1 = \int_0^{\frac{1}{2}\pi}\left\langle a\frac{\partial}{\partial r}\Phi_0^1\right\rangle \cos(2n-2)\theta\ \mathrm{d}\theta = -\frac{\pi}{4}\frac{(Ka)^{2n-2}}{(2n-3)!}G_{2n-3} + \sum_{j=0}^{\infty}\frac{(Ka)^{2j+1}}{(2j)!}G_{2j}\frac{(2j+1)(-1)^{n+j}}{4(n-1)^2-(2j+1)^2} + \frac{1}{2}\sum_{j=1}^{\infty}\frac{(-Ka)^j}{(j-1)!}(S_{j+2n-2}+S_{j-2n+2})$$

for $n > 1$, and

$$A_{n1}^2 = \int_0^{\frac{1}{2}\pi}\left\langle a\frac{\partial}{\partial r}\Phi_0^2\right\rangle \sin(2n-1)\theta\ \mathrm{d}\theta = -\frac{\pi}{4Ka}\delta_{1n} - \frac{\pi}{4}\frac{(Ka)^{2n-1}}{(2n-2)!}G_{2n-2} + \sum_{j=0}^{\infty}\frac{(Ka)^{2j+1}}{(2j+1)!}G_{2j+1}\frac{(2j+2)(-1)^{n+j}}{(2n-1)^2-4(j+1)^2} + \frac{1}{2}\sum_{j=1}^{\infty}\frac{(-Ka)^j}{(j-1)!}(S_{2n-1+j}+S_{2n-1-j})$$

for $n \geqslant 1$. Here,

$$G_0 = \log Ka - i\pi + \gamma \quad G_m = G_{m-1} - 1/m \quad \text{for } m > 0$$

$$S_m = \int_0^{\frac{1}{2}\pi}\theta\sin m\theta\ \mathrm{d}\theta = \{\sin(\tfrac{1}{2}m\pi) - \tfrac{1}{2}m\pi\cos(\tfrac{1}{2}m\pi)\}/m^2$$

and $S_0 = 0$. Note that A_{nm}^σ are real for $m > 1$.

Now

$$b_n^1 = \int_0^{\frac{1}{2}\pi}\left\langle a\frac{\partial}{\partial r}[-\exp(-Ky)\cos Kx]\right\rangle \cos(2n-2)\theta\ \mathrm{d}\theta$$

and

$$b_n^2 = \int_0^{\frac{1}{2}\pi}\left\langle a\frac{\partial}{\partial r}[i\exp(-Ky)\sin Kx]\right\rangle \sin(2n-1)\theta\ \mathrm{d}\theta$$

i.e. b_n^1 is real and b_n^2 is imaginary. We have $b_1^1 = \sin Ka$

$$b_n^1 = -\frac{\pi}{4}\frac{(Ka)^{2n-2}}{(2n-3)!} + \sum_{j=0}^{\infty}\frac{(Ka)^{2j+1}}{(2j)!}\frac{(2j+1)(-1)^{n+j}}{4(n-1)^2-(2j+1)^2}$$

for $n > 1$, and

$$b_n^2 = i\frac{\pi}{4}\frac{(Ka)^{2n-1}}{(2n-2)!} - i\sum_{j=0}^{\infty}\frac{(Ka)^{2j+2}}{(2j+1)!}\frac{(2j+2)(-1)^{n+j}}{(2n-1)^2-4(j+1)^2}$$

for $n \geqslant 1$. This completes the specification of the matrix elements.

Force coefficients. By symmetry, we have

$$f_x = \frac{-2i\omega}{Ag}\int_0^{\frac{1}{2}\pi}\langle\phi_I^2+\phi_D^2\rangle\sin\theta\ \mathrm{d}\theta$$

and

$$f_y = \frac{-2i\omega}{Ag}\int_0^{\frac{1}{2}\pi}\langle\phi_I^1+\phi_D^1\rangle\cos\theta\ \mathrm{d}\theta$$

Now

$$\frac{\omega}{Ag}\int_0^{\frac{1}{2}\pi}\langle\phi_I^1\rangle\cos\theta\,\mathrm{d}\theta = 1-\frac{1}{4}\pi Ka-\sum_{j=1}^{\infty}\frac{(Ka)^{2j}}{(2j)!}\frac{(-1)^j}{(4j-1)}$$

and

$$\frac{\omega}{Ag}\int_0^{\frac{1}{2}\pi}\langle\phi_I^2\rangle\sin\theta\,\mathrm{d}\theta = -\frac{1}{4}i\pi Ka-i\sum_{j=1}^{\infty}\frac{(Ka)^{2j}}{(2j-1)!}\frac{(-1)^j}{(4j^2-1)}$$

Using equation (3.2) (truncated at $m=N-1$), we also find that

$$\frac{\omega}{Ag}\int_0^{\frac{1}{2}\pi}\langle\phi_D^1\rangle\cos\theta\,\mathrm{d}\theta$$

$$= c_1^1\Psi_1+\frac{1}{4}\pi Kac_2^1+\sum_{m=2}^{N}c_m^1\frac{(-1)^m}{4(m-1)^2-1}$$

and

$$\frac{\omega}{Ag}\int_0^{\frac{1}{2}\pi}\langle\phi_D^2\rangle\sin\theta\,\mathrm{d}\theta$$

$$= c_1^2\Psi_2+Ka\sum_{m=2}^{N}c_m^2\frac{(-1)^m}{4(m-1)^2-1}$$

where

$$\Psi_1=\int_0^{\frac{1}{2}\pi}\langle\Phi_0^1\rangle\cos\theta\,\mathrm{d}\theta$$

and

$$\Psi_2=\int_0^{\frac{1}{2}\pi}\langle\Phi_0^2\rangle\sin\theta\,\mathrm{d}\theta$$

$$\Psi_1=-G_0+\frac{1}{4}\pi KaG_1+\sum_{j=1}^{\infty}\frac{(Ka)^{2j}}{(2j)!}G_{2j}\frac{(-1)^j}{(4j^2-1)}$$

$$+\frac{1}{2}\sum_{j=1}^{\infty}\frac{(-Ka)^j}{j!}\{S_{j+1}+S_{j-1}\}$$

and

$$\Psi_2=1+\frac{1}{4}\pi\{(Ka)^{-1}-KaG_1\}-\sum_{j=1}^{\infty}\frac{(Ka)^{2j}}{(2j-1)!}G_{2j}\frac{(-1)^j}{(4j^2-1)}$$

$$+\frac{1}{2}\sum_{j=1}^{\infty}\frac{(-Ka)^j}{j!}\{S_{1+j}+S_{1-j}\}$$

APPENDIX B

For x sufficiently large, the surface elevation ahead of the cylinder is given by equation (2.7), as

$$\eta(x) = -iA\,[\exp(-iKx)+R\,\exp(iKx)]$$

Write $\eta(x_A)=\eta_A$ and $R=|R|\exp(i\delta)$, whence

$$|\eta_A|^2=|A|^2\{1+|R|^2+2|R|\cos(2Kx_A+\delta)\}$$

Let $x_B=x_A\pm\frac{1}{4}L$, where the wavelength, $L=2\pi/K$. Then

$$|\eta_B|^2=|A|^2\{1+|R|^2-2|R|\cos(2Kx_A+\delta)\}$$

where $\eta_B=\eta(x_B)$. Thus

$$(|\eta_A|\pm|\eta_B|)^2=2|A|^2\{1+|R|^2\pm((1+|R|^2)^2-4|R|^2\cos^2(2Kx+\delta))^{1/2}\}$$

whence

$$\min\{(|\eta_A|+|\eta_B|)^2\}=4|A|^2$$

and

$$\max\{(|\eta_A|-|\eta_B|)^2\}=4|A|^2|R|^2$$

both of these occurring at the same value of x_A.